International Journal of Technology (2018) 2: 412-421
ISSN 2086-9614

SIMULATION OF A METAL ORGANIC FRAMEWORK-BASED ADSORBED NATURAL GAS STORAGE TANK

Yuswan Muharam[1*], Eny Kusrini[1], Nurainia Saubryani[1], Maria Ulfa[1]

[1]*Department of Chemical Engineering, Faculty of Engineering, Universitas Indonesia, Kampus UI Depok, Depok 16424, Indonesia*

(Received: December 2017 / Revised: January 2018 / Accepted: January 2018)

ABSTRACT

An adsorbed natural gas storage tank was simulated in this work, with the objective being to predict the filling time, the filling capacity and the storage efficiency. A high-capacity HKUST-1 type metal-organic framework was used as adsorbent. The time-dependent phenomenological model of the adsorbed natural gas storage tank was developed considering mass, momentum and energy transfers. The cylindrical tank was 1.09 m in length with a radius of 0.15 m, and was equipped with an inlet hole for gas inflow. The simulation results show that the temperature increase in the tank due to adsorption heat is very significant. This affects the adsorption ability of the bed inside the tank, so the storage efficiency is consequently low. For the inlet gas flowrate of 50 L/min, the storage efficiency is 38% and increases to only 47% at 5 L/min. Corresponding filling capacities for the two flowrates are not very different, i.e. 89 V(STP)/V and 109 V(STP)/V. However, the difference in the filling times is extremely significant, which are 16 min at 50 L/min and 255 min at 5 L/min.

Keywords: Adsorbed natural gas; Metal-organic frameworks; Simulation; Storage tank

1. INTRODUCTION

One of currently emerging gas storage technologies is natural gas adsorption using porous adsorbents, known as adsorbed natural gas (ANG) (Vasiliev et al., 2000; Bastos-Neto et al., 2005). The technology requires no liquefaction or multistage compression processes. In ANG technology, natural gas is held in a porous material (adsorbent) at a pressure of 35 atm – 40 atm (Pupier et al., 2005). The energy density of ANG at 35 atm is proportional to that of CNG at 165 atm (Nie et al., 2016).

The performance of ANG storage is affected by the nature of the microporous solid (Biloe et al., 2002; Lozano-Castelló et al., 2002a; Lozano-Castelló et al., 2002b), the adsorbent size (MacDonald & Quinn, 1998; Biloe et al., 2001a), the scale of the ANG storage tank (Chang & Talu, 1996; Biloe et al., 2001b), the natural gas composition (Seki & Sumie, 2001; Pupier et al., 2005), and the inlet flowrate (Sahoo et al., 2011; Alhamid et al., 2015). During the filling process of natural gas into a storage tank, the gas undergoes several process stages, each of which has a mass transfer resistance that decreases the storage capacity. In addition, the heat released during the adsorption process leads to an increase in the temperature inside the tank, thereby reducing the storage capacity.

The U.S. Department of Energy has set the total uptake of ANG at 263 V(STP)/V. Experimental research has been conducted by Peng et al. (2013) to achieve the target using a HKUST-1 type

*Corresponding author's email: muharam@che.ui.ac.id, Tel. +62-21-7863576, Fax. +62-21-7863515
Permalink/DOI: https://dx.doi.org/10.14716/ijtech.v9i2.1100

metal-organic framework (MOF) adsorbent. At 65 atm and 298 K, the total methane uptake if the bed efficiency loss is ignored reaches 267 V(STP)/V, or equivalent to that of CNG at 255 atm. However, when this adsorbent is applied in a storage tank, the total methane uptake decreases due to the heat-released and mass transfer resistances. Therefore, the performance of the adsorbent in an ANG storage tank needs to be tested, either experimentally or through computer simulation, to discover the total methane uptake.

Computer simulation is a fast and efficient way to determine the performance of a system (Muharam & Kurniawan, 2016). In the case of ANG storage tanks, it predicts filling characteristics such as storage capacity, storage efficiency and filling time, which are affected by temperature rises and mass transfer resistances in the tanks.

Simulation of an ANG storage tank using Norit RGM1 activated carbon adsorbent has been performed by Sahoo et al. (2011). Their 2-dimensional axisymmetric model considers mass, energy and momentum transfers. The calculated natural gas storage capacity for the constant filling flowrate of 1 L/min and the filling time of 120 min is 72.5 V(STP)/V, while the value of the equilibrium storage capacity is 80.6 V(STP)/V. The maximum temperature increase achieved in the tank during filling is 27 K.

Simulation of an ANG storage tank using HKUST-1 type metal-organic framework adsorbent has not been carried out. Therefore, the objective of the present work is to predict the filling characteristics such as filling time, filling capacity and storage efficiency of an ANG storage tank, with HKUST-1 as adsorbent, through computer simulation.

2. METHODS

In order to achieve the objective, a 2-dimensional phenomenological axisymmetric model of an ANG storage tank was developed and solved numerically using COMSOL Multiphysics. The model considers mass, energy and momentum transfers to meet high accuracy prediction.

The system of the ANG storage tank is a cylindrical tank, as illustrated in Figure 1. Natural gas enters the tank through a small hole in the front of a smaller cylinder at the upstream of the tank. The tank consists of two different-size cylinders. The larger cylinder has a radius, R_{ls}, of 0.15 m, and a height, L_{ls} of 1.09 m. The smaller cylinder has a radius, R_{ss}, of 0.04 m, and a height, L_{ss} of 0.14 m. The inlet hole has a radius, R_{io}, of 0.01 m. The two cylinders are filled by porous adsorbent particles as a so-called fixed bed. Natural gas enters through the inlet hole at a constant flow rate Q_{in} and constant temperature T_{in}. Since the gas is assumed to be a single component of methane, it is transported into the bed interstices by convection. For the same reason, no internal diffusion limitation occurs in the particle pores, so the gas is immediately adsorbed onto the adsorbent surfaces when it is in the pores. The adsorbed gas is in equilibrium with the gaseous state. The energy released heats up the bed. Heat removal from the bed is performed by setting the tank wall at a certain temperature.

The total mass balance through a porous medium is described by the following equation:

$$\frac{\partial(\varepsilon_t \rho_g + a_{eq})}{\partial t} + \frac{1}{r}\frac{\partial(r\rho_g U_r)}{\partial r} + \frac{\partial(\rho_g U_z)}{\partial z} = 0 \quad (1)$$

where ε_t is total porosity and ρ_g is gas density.

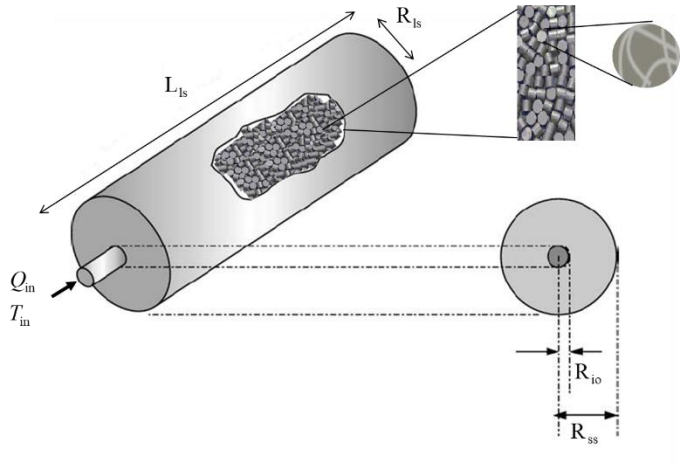

Figure 1 Model of ANG storage tank

The axial and radial velocities are defined by Darcy's law, as follows:

$$U_z = -\frac{\kappa}{\mu}\frac{\partial P}{\partial z} \tag{2}$$

$$U_r = -\frac{\kappa}{\mu}\frac{\partial P}{\partial r} \tag{3}$$

where μ is gas dynamic viscosity, and P is pressure.

The porous media permeability, κ, is calculated using the Carman-Kozeny equation (Sahoo et al., 2011):

$$\kappa = \frac{4\varepsilon_b r_p^{\ 2}}{150(1-\varepsilon_b)^2} \tag{4}$$

where ε_b is bed porosity and r_p is adsorbent radius.

The total methane intake at standard temperature and pressure (STP), a_{eq}, is formulated as follows:

$$\frac{a_{eq}}{C_0} = \frac{k_0 \exp\left(\frac{\Delta H_{ads}}{RT}\right)P}{1 + k_0 \exp\left(\frac{\Delta H_{ads}}{RT}\right)P} \tag{5}$$

where k_0, ΔH_{ads} and C_0 for the HKUST-1 adsorbent were obtained by the regression of the experimental data from Peng et al. (2013).

The heat balance in the ANG storage tank is

$$(\rho C_p)_{eff}\frac{\partial T}{\partial t} + \rho C_p\left(u_r\frac{\partial T}{\partial r} + u_z\frac{\partial T}{\partial z}\right) - \left(\frac{1}{r}\frac{\partial}{\partial r}\left(rk_{er}\frac{\partial T}{\partial r}\right) + \frac{\partial}{\partial z}\left(k_{ez}\frac{\partial T}{\partial z}\right)\right) = Q \tag{6}$$

where $(\rho C_p)_{eff}$ is effective heat capacity, k_{er} radial effective heat conductivity, and k_{ez} axial effective heat conductivity.

The adsorption heat, Q, is formulated by

$$Q = \frac{\partial\left(\Delta H_{ads}\frac{P_{STP}}{P}\frac{T}{T_{STP}}\frac{\rho_g a_{eq}}{M_g}\right)}{\partial t} \tag{7}$$

where M_g is gas molecular weight, and T_{STP} and P_{STP} are standard temperature and pressure (273.15 K, 1 atm).

For the mass transfer equation, all the boundary conditions at the wall are no flux. The boundary condition at the inlet hole is inlet velocity, v_{inlet}.

For the heat transfer equation, all the boundary conditions at the wall are

$$k_{er}\frac{\partial T}{\partial r} = h(T_{cxt} - T) \tag{8}$$

where T_{ext} is the wall temperature.

The boundary condition at the inlet hole is

$$k_{ez}\frac{\partial T}{\partial z} = \rho_g v_0 \int_{T_{inlet}}^{T} C_p dT \tag{9}$$

where v_0 is inlet superficial velocity.

The heat transfer coefficient across the bed-wall interface, h, is

$$h = \frac{\mathrm{Nu}_w k_g}{d_p} \tag{10}$$

where k_g is gas heat conductivity, and d_p is adsorbent diameter.

The Nusselt number, Nu_w, was formulated by Paterson & Carberry (1983) as:

$$\mathrm{Nu}_w = 5.73\left(\frac{D_t}{d_p}\right)^{0.5}\frac{\mathrm{Pr}\left(0.11\mathrm{Re}_p + 20.64\right)}{\mathrm{Re}_p^{0.262}} \tag{11}$$

where D_t is tank diameter.

The Reynolds number, Re_p, is as follows:

$$\mathrm{Re}_p = \frac{\rho_g v_s d_p}{\mu\left(1-\varepsilon_b\right)} \tag{12}$$

where v_s is superficial velocity.

The initial values at $t = 0$ are $P = 1$ atm and $T = 298.15$ K.

3. RESULTS AND DISCUSSION

3.1. Filling Characteristics

The simulation was carried out to predict filling time, filling capacity and storage efficiency. Filling time is defined as the time in which the bed pressure reaches 35 atm. Filling capacity is the total natural gas volume in the tank in a gaseous and adsorbed state when filling is completed. Storage efficiency is defined as the ratio of filling capacity to maximum capacity at inlet temperature and 35 atm.

The simulation indicates that for an inlet flowrate of 50 L/min and inlet temperature of 298.15 K, the filling time is 17.4 min and filling capacity is 97.78 V(STP)/V. Figure 2 shows the pressure

distribution in the tank at three different times: 5 min, 10 min and filling time. It can be seen that pressure is almost evenly distributed in the tank from the beginning of the filling. This occurs because natural gas is assumed to be a single component and its transportation in the bed interstices is only by convection. No mixing happens, as is the case for multicomponent systems.

Figure 3 shows the temperature distribution in the bed. The increase in temperature immediately takes place when heat is released. The amount of heat released is proportional to the amount of gas adsorbed. At 5 minutes and 10 minutes, the maximum temperature increases are 23 K and 54 K, while at the filling time, the maximum temperature increase is 169 K. This situation takes into account cooling from the tank wall, since it was set to 298 K. This indicates that the cooling across the tank is ineffective, as it is a packed-bed characteristic. When compared to the simulation results obtained by Sahoo et al. (2011) with Norit RGM1, the maximum temperature increase in this study is much higher. In addition to the higher methane adsorption rate on HKUST-1, which consequently contributes to the higher heat release rate, the thermal conductivity of MOF is about 0.3 W/m.K (Huang et al., 2007), which is lower than that of Norit RGM1.

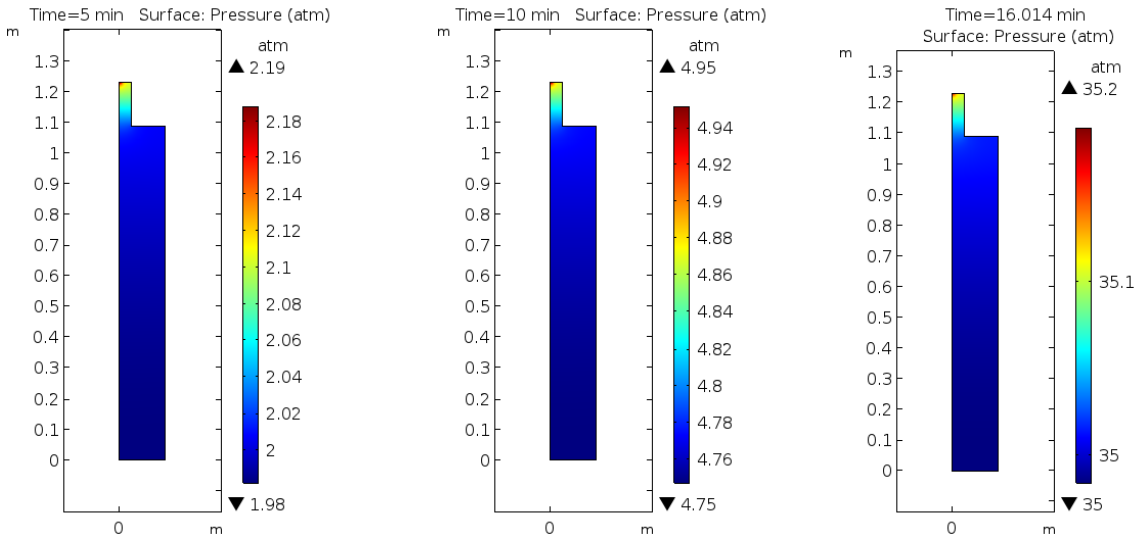

Figure 2 Pressure distribution for Q_{in} = 50 L/min

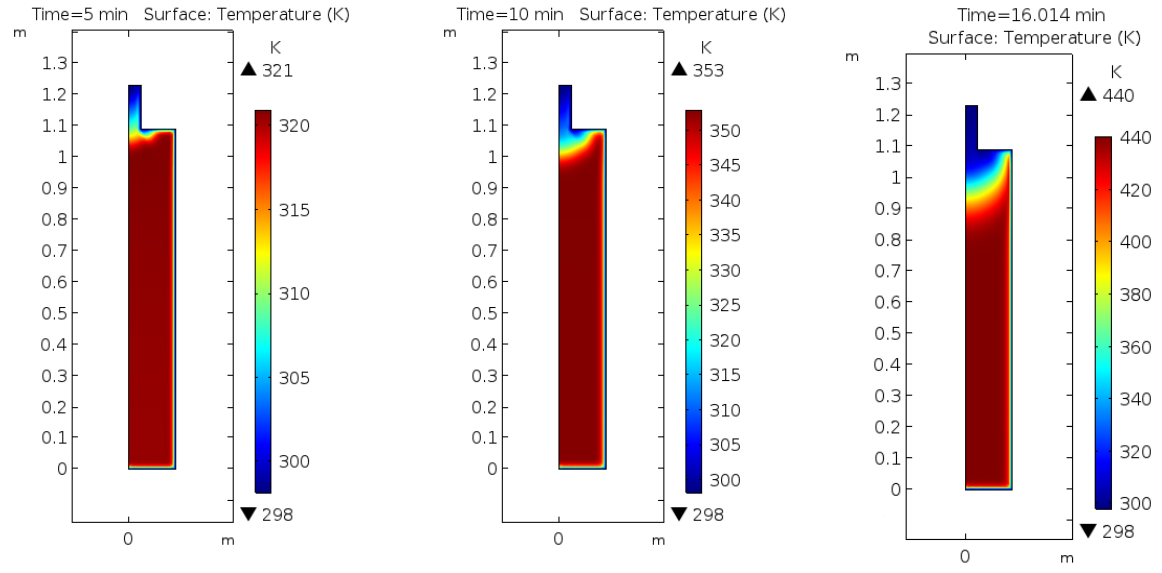

Figure 3 Temperature distribution for Q_{in} = 50 L/min

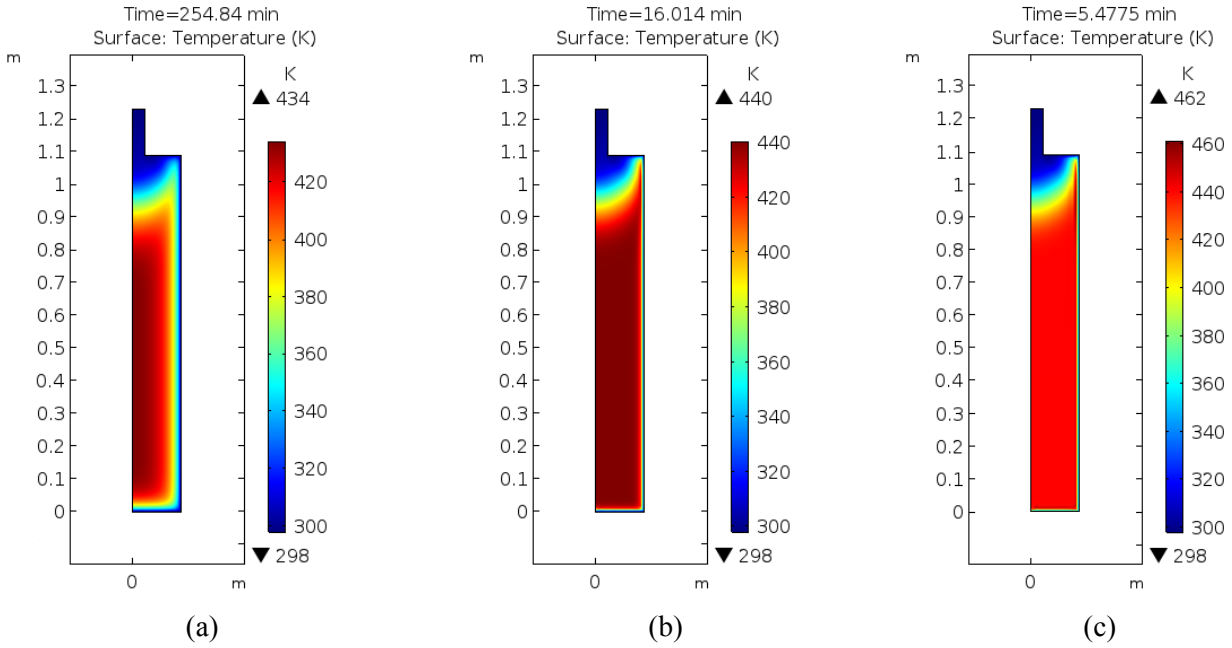

Figure 4 Temperature distribution for: (a) Q_{in} = 5 L/min; (b) Q_{in} = 50 L/min; and (c) Q_{in} = 125 L/min at each filling time

The temperature distribution in the bed at 5 L/min, 50 L/min and 125 L/min for each filling time is shown in Figure 4. The temperature distribution pattern for the three flowrates is nearly the same. The higher temperature occurs in the rear section of the bed and the heat released in the front section of the bed is conveyed by the flowing gas to the rear and accumulates there, so the temperature in the rear section is higher. For higher flowrates, the maximum temperature increase is higher than for the lower ones. This is because the fluid mass in the bed increases more quickly when the flowrate is faster, resulting in a faster increase in pressure. Accordingly, the heat release due to adsorption is faster. These two factors, i.e. convective heat and adsorption heat, lead to a rapid temperature rise for high flowrates. At 5 L/min and 125 L/min, the maximum temperature increases are 136 K and 164 K respectively.

The increase in pressure is slow at the beginning of the filling, as shown in Figure 5 for 5 L/min. The pressure gradient soars towards the end of the filling, i.e. after 225 minutes. However, this is not accompanied by a soaring of the adsorbed gas volume at the same time, as shown in Figure 6. This is because the increase in pressure is also accompanied by an increase in temperature, as seen in Figure 7. When compared to the experimental results in an isothermal condition, i.e. 298 K, the increase in the total gas intake has a lower gradient than the isothermal condition, as shown in Figure 8. The efficiency loss increases with increasing pressure.

The gas stored in the tank consists of two states: adsorbed and gaseous. Since the final pressure inside the tube is set to 35 atm, the gaseous state volume per tank volume is the same, regardless of the flowrate. The simulation result shows that the gaseous state volume is 20 V(STP)/V, which contributes 22% of the total gas volume for high flowrates. As shown in Figure 9, the adsorbed state volume is high for the flowrate below 10 L/min. At 5 L/min, the adsorbed state volume is 88 V (STP)/V and the total gas volume is 109 V (STP)/V. At flowrates above 10 L/min, the temperature effect on the adsorbed state volume is significant.

The profiles of the storage efficiency and filling time are shown in Figures 10 and 11. They have the same trend, in which both the storage efficiency and the filling time increase significantly when the flowrate decreases in the range below 20 L/min. A lower flowrate leads to a longer

filling time. However, the storage efficiency is sufficiently high. In order to achieve a filling capacity of 109 V(STP)/V, the flowrate should be 5 L/min, with a filling time of 255 min. In these conditions, storage efficiency is 47%.

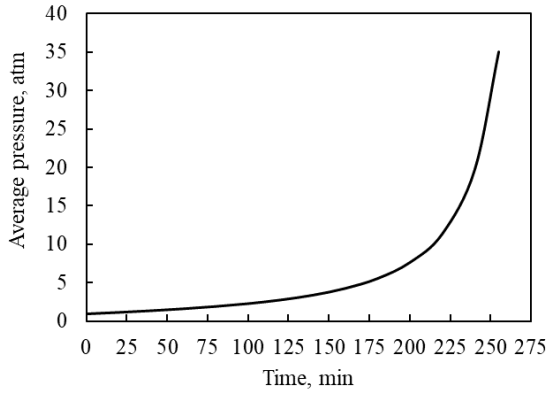

Figure 5 Pressure dynamics inside the bed

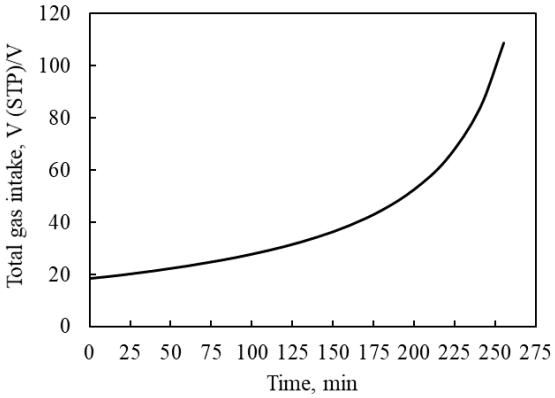

Figure 6 Total gas intake inside the bed

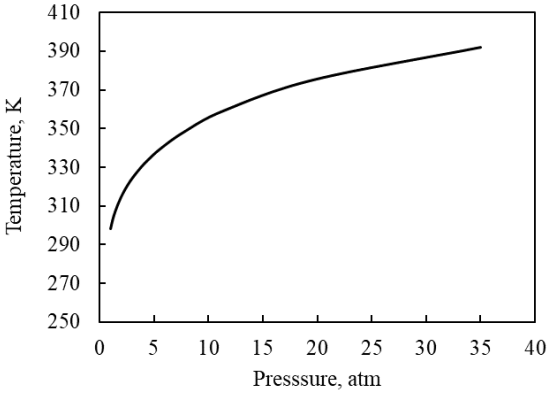

Figure 7 Temperature vs pressure

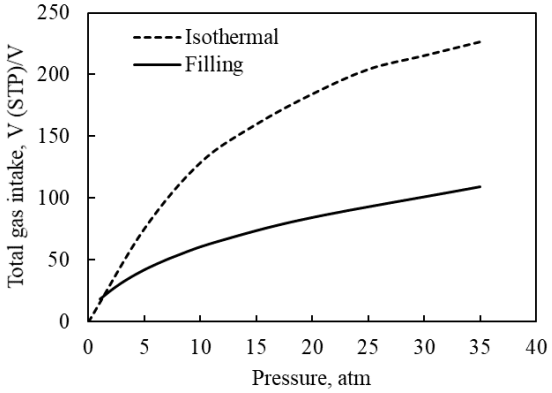

Figure 8 Isothermal and filling gas intakes

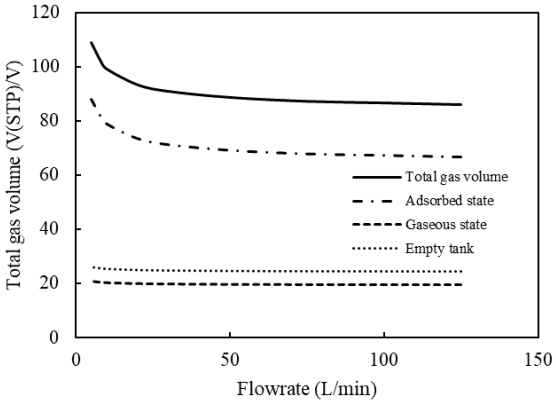

Figure 9 Filling capacity at various flowrates

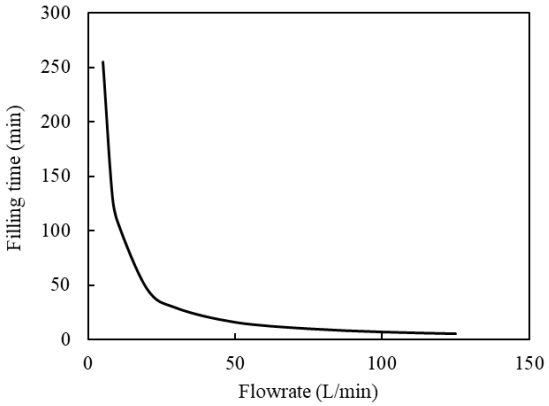

Figure 10 Storage efficiency at various flowrates

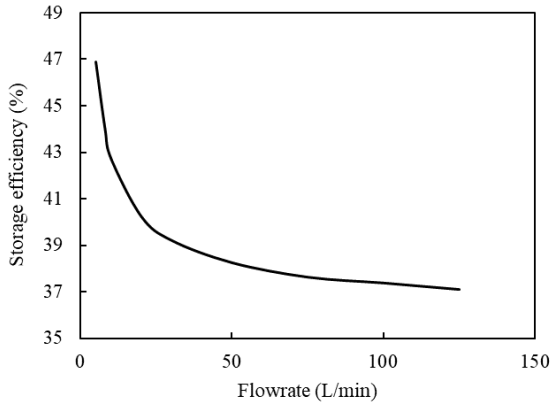

Figure 11 Filling time at various flowrates

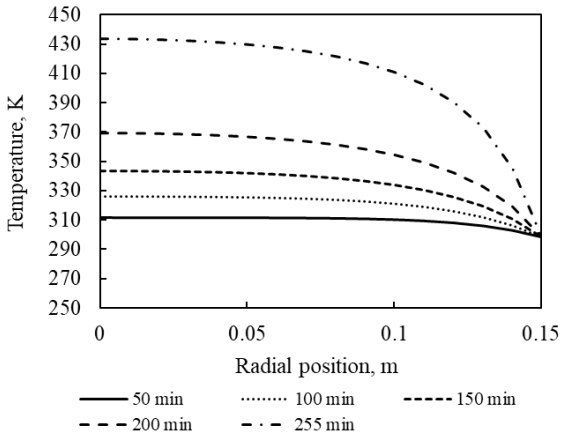

Figure 12 Temperature dynamics in the radial direction

3.2. Cooling Effectiveness

Storage efficiency will be high if the bed temperature is close to the inlet gas temperature. The temperature increase inside the bed can be suppressed by cooling using cooling media. Four heat transfer resistances are present during heat removal from the bed to the cooling media: bed conductive resistance; bed-wall thermal boundary layer; wall conductive resistance; and wall-cooling media boundary layer. The latter can be suppressed by the convective flow of the cooling media. Wall conductive resistance can be minimized by the selection of appropriate materials, while the bed-wall thermal boundary layer can be suppressed by arranging the porous matrix properties. Bed conductive resistance can be diminished by using an adsorbent with high thermal conductivity. Therefore, researches on adsorbents for natural gas storage do not only focus on adsorbents with a high adsorption capacity, but also high cycle usage and high thermal conductivity.

In this study, bed conductive resistance can be ascertained from the temperature profile in the radial direction. Figure 12 presents the dynamic temperature profile in the radial direction at a particular axial position for 5 L/min. As can be seen in the figure, the cooling process has been continuous since the beginning of the filling. The increasing temperature with time indicates that the bed heating rate dominates the cooling rate. The low thermal conductivity of the adsorbent material leads to low molecular heat transfer. The cooling is practically successful up to about 3 cm from the tube wall. This is the reason for increasing the aspect ratio (length to diameter) of the tank for effective cooling. However, cooling effectiveness remains an area of study because of the competition between good cooling with a high aspect ratio and high temperature increase due to high gas adsorption. Gas adsorbed at a temperature which is still low will be desorbed when the temperature increases due to the heat released, which is a quite complicated process.

4. CONCLUSION

The high-capacity HKUST-1 type metal-organic framework was used as the adsorbent in the adsorbed natural gas storage tank in this simulation work. It loses efficiency by more than 50% during filling due to the high temperature increase. At an inlet gas flowrate of 50 L/min, the storage efficiency is 38% and increases to only 47% at 5 L/min. The filling capacities for the two flowrates are not very different. However, the difference in the filling times is very significant.

5. ACKNOWLEDGEMENT

We express our gratitude to the University of Indonesia, which funded this research through the *Hibah Publikasi Internasional Terindeks untuk Tugas Akhir Mahasiswa* (PITTA 2017) No 864/UN2.R3.1/HKP.05.00/2017 scheme.

6. REFERENCES

Alhamid, M.I., Nasruddin, Senoadi, Perdana, M.B., Ratiko, 2015. Effect of Methane Gas Flowrate on Adsorption Capacity and Temperature Distribution of Activated Carbon. *International Journal of Technology*, Volume 6(4), pp. 584–593

Bastos-Neto, M., Torres, A.E.B., Azevado, D.C.S., Cavalcante Jr., C.L., 2005. A Theoretical and Experimental Study of Charge and Discharge Cycles in a Storage Vessel for Adsorbed Natural Gas, *Adsorption*, Volume 11(2), pp. 147–157

Biloe, S., Goetz, V., Guillot, A., 2002. Optimal Design of an Activated Carbon for an Adsorbed Natural Gas Storage System. *Carbon*, Volume 40(8), pp. 1295–1308

Biloe, S., Goetz, V., Mauran, S., 2001a. Characterization of Adsorbent Composite Blocks for Methane Storage. *Carbon*, Volume 39(11), pp. 1653–1662

Biloe, S., Goetz, V., Mauran, S., 2001b. Dynamic Discharge and Performance of a New Adsorbent for Natural Gas Storage. *AIChE Journal*, Volume 47(12), pp. 2819–2830

Chang, K.J., Talu, O., 1996. Behavior and Performance of Adsorptive Natural Gas Storage Cylinders during Discharge. *Applied Thermal Engineering*, Volume 16(5), pp. 359–374

Huang, B.L., McGaughey, A.J.H., Kaviany, M., 2007. Thermal Conductivity of Metal-organic Framework 5 (MOF-5): Part I. Molecular Dynamics Simulations. *International Journal of Heat and Mass Transfer*, Volume 50(3-4), pp. 393–404

Lozano-Castelló, D., Cazorla-Amorós, D., Linares-Solano, A., 2002a. Can Highly Activated Carbons be Prepared with a Homogeneous Micropore Size Distribution? *Fuel Processing Technology*, Volume 77-78, pp. 325–330

Lozano-Castelló, D., Cazorla-Amoros, D., Linares-Solano, A., Quinn, D.F., 2002b. Influence of Pore Size Distribution on Methane Storage at Relatively Low Pressure: Preparation of Activated Carbon with Optimum Pore Size. *Carbon*, Volume 40(7), pp. 989–1002

MacDonald, J.A.F., Quinn, D.F., 1998. Carbon Absorbents for Natural Gas Storage. *Fuel*, Volume 77(1), pp. 61–64

Muharam, Y., Kurniawan, A., 2016. Computational Fluid Dynamic Application in Scale-up of a Stirred-batch Reactor for Degumming Crude Palm Oil. *International Journal of Technology*, Volume 7(8), pp. 1344–1351

Nie, Z., Lin, Y., Jin, X., 2016. Research on the Theory and Application of Adsorbed Natural Gas Used in New Energy Vehicles: A Review. *Frontiers of Mechanical Engineering*, Volume 11(3), pp. 258–274

Paterson, W.R., Carberry, J.J., 1983. Fixed Bed Catalytic Reactor Modelling: The Heat Transfer Problem. *Chemical Engineering Science*, Volume 38(1), pp. 175–180

Peng, Y., Krungleviciute, V., Eryazici, I., Hupp, J.T., Farha, O.K., Yildirim, T., 2013. Methane Storage in Metal–organic Frameworks: Current Records, Surprise Findings, and Challenges. *Journal of the American Chemical Society*, Volume 135(32), pp. 11887–11894

Pupier, O., Goetz, V., Fiscal, R., 2005. Effect of Cycling Operations on an Adsorbed Natural Gas Storage. *Chemical Engineering and Processing: Process Intensification*, Volume 44(1), pp. 71–79

Sahoo, P.K., John, M., Newalkar, B.L., Choudhary, N.V., Ayappa, K.G., 2011. Filling Characteristics for an Activated Carbon Based Adsorbed Natural Gas Storage System. *Industrial & Engineering Chemistry Research*, Volume 50(23), pp. 13000–13011

Seki, K., Sumie, Y., 2001. Development of Adsorptive Natural Gas Storage System – Application to Gas Holder and Natural Gas Vehicle. *In*: Proceedings of IGRC, Amsterdam, pp. 308–315

Vasiliev, L.L., Kanonchik, L.E., Mishkinis, D.A., Rabetsky, M.I., 2000. Adsorbed Natural Gas Storage and Transportation Vessels. *International Journal of Thermal Sciences*, Volume 39(9-11), pp. 1047–1055